Seismic performance of multi-storey steel frame buildings with various configurations of eccentric braced

Inka Nabilla[1], *Ridho* Aidil Fitrah[1*], and *Masrilayanti* Masrilayanti[1]

[1]Department of Civil Engineering, Faculty of Engineering, Universitas Andalas, Padang, Indonesia

Abstract. Structural stability and strength are essential to ensure adequate seismic performance particularly for Eccentrically Braced Frames (EBF) by providing high elastic stiffness, ductility, and energy dissipation. This study analyses the optimal configuration of EBF system for industrial buildings using nonlinear static pushover analysis. Four structural models were analyzed: one unbraced as a baseline and three EBF configurations with varying bracing placements, considering both service and earthquake load conditions. Fragility curves were then derived from capacity curve, incorporating key parameters such as yield and ultimate roof displacement. The findings indicate differences in seismic performance among the models. Model-A shows early onset of damage and collapse, reflecting limited ductility. Model B performs better but less reliable at higher damage states. Model C and D demonstrate adequate resilience, with delayed damage progression and higher ultimate displacement capacity. It was concluded that the most optimum eccentric bracing configuration is model B (model with bracing installed on all exterior sides of the structure) because it is suitable for service-level performance, while model D (model with bracing installed on center of exterior of the structure) provides the greatest safety against collapse, making it the most reliable for building in high seismic regions.

1 Introduction

A well-designed structure must exhibit stability, strength, and constructability. Structural stability refers to the ability of a building to resist damage and maintain functionality under service conditions. Meanwhile, a structure must ensure to remain standing and not experience a hazard when subjected to its ultimate limit state. Serviceability and ultimate limit state are influenced by various factors, one of which is natural hazards [1, 2]. This is a crucial issue to consider when planning buildings in Indonesia, which is located along the Pacific Ring of Fire, where seismic activity is frequent and severe. Consequently, the design and selection of an appropriate lateral load-resisting system become vital to enhancing structural stability and strength, ensuring that buildings remain safe and serviceable throughout their lifespan [3, 4].

The Eccentrically Braced Frame (EBF) structural system represents an advanced development in steel-seismic-resisting systems, combining the advantages of the Moment-Resisting Frame (MRF) and the Concentrically Braced Frame (CBF) while mitigating the limitations inherent in both systems. The MRF system is characterized by its excellent ductility but often lacks sufficient stiffness, leading to excessive lateral drift under seismic loading[5, 6]. In contrast, the CBF system provides high lateral stiffness and strength but exhibits limited ductility and energy dissipation capacity du to the concentration of axial forces in the braces, which can result in brittle failure modes during strong earthquakes.

However. The EBF system effectively bridges these two approaches by providing both high elastic stiffness and significant ductility. In an EBF, a short beam segment known as the link beams is installed between the ends of the braces and the main beam. This link beam is designed to deform inelastically during seismic excitation, while the surrounding structural components. The controlled yielding of the link beam serves as primary mechanism for energy dissipation, thereby protecting the overall structural integrity [7, 8]. Numerous experimental and analytical studies have confirmed that EBF system exhibit superior performance under cyclic and dynamic loading compared to conventional braced or moment-resisting frames [7, 9, 10]. The high energy dissipation capacity and stable hysteretic behavior of the EBF make it one of the most reliable and cost-effective solutions for earthquake-resistant steel buildings.

Although the EBF system has been proven to provide adequate seismic performance through its essential strength and ductility, its effectiveness is highly dependent on the configuration and placement of the bracing within the structure [11]. The geometry and distribution of the braces along the plan and elevation of buildings influence the stiffness distribution, plastic hinge formation, and probability to experience certain damage. Furthermore, the seismic performance of each EBF configuration probably diverse depending on its intended design objective. As a result, each configuration serves a

* Corresponding author: ridho@eng.unand.ac.id

distinct structural purpose highlighting the importance of selecting an appropriate configuration that aligns with the desired performance level and seismic design criteria [12].

This study aims to evaluate the seismic performance of various configurations of EBF applied to industrial steel frame buildings, with the objective of identifying the most effective configuration for protecting the main structural system. Specifically, the research investigates how different EBF configurations influence the structural response characteristic, including strength, stiffness, ductility, performance level, under seismic loading conditions through appropriate method.

2 Methodology

2.1 Building modelling and section properties

The building modelled in this study is an eight-storey industrial structured framed in steel with its layout for each floor illustrated in Fig. 1. The primary lateral-resisting system investigated is the Eccentrically Braced Frame (EBF) using a split-K bracing arrangement with a short link beam length of 500 mm. Five structural member types (columns, beams, secondary beams, bracing, and link beam) were assigned to model in Table 1 and previously checked to adequate the design criteria through auto-select features in ETABS v18.

Table 1. Structural cross-sectional profiles.

Structure	Profile	Grade
Column	**WF 307.305.10.15** (A = 11920 mm^2; Ix 2.12 x 10^8 mm^4)	ASTM A36 fy=250 MPa, fu=410 MPa
Beam	**WF 307.205.9.15** (A = 8643 mm^2; Ix 1.47 x 10^8 mm^4)	
Secondary beam	**WF 247.202.7.11** (A = 6019 mm^2; Ix 6.85 x 10^7 mm^4)	
Bracing	**WF 201.215.6.10** (A = 5386 mm^2; Ix 4.22 x 10^7 mm^4)	ASTM A36 fy=210 MPa, fu=340 MPa
Link beam	**WF 310.102.6.9** (A = 3588 mm^2; Ix 5.4 x 10^7 mm^4)	

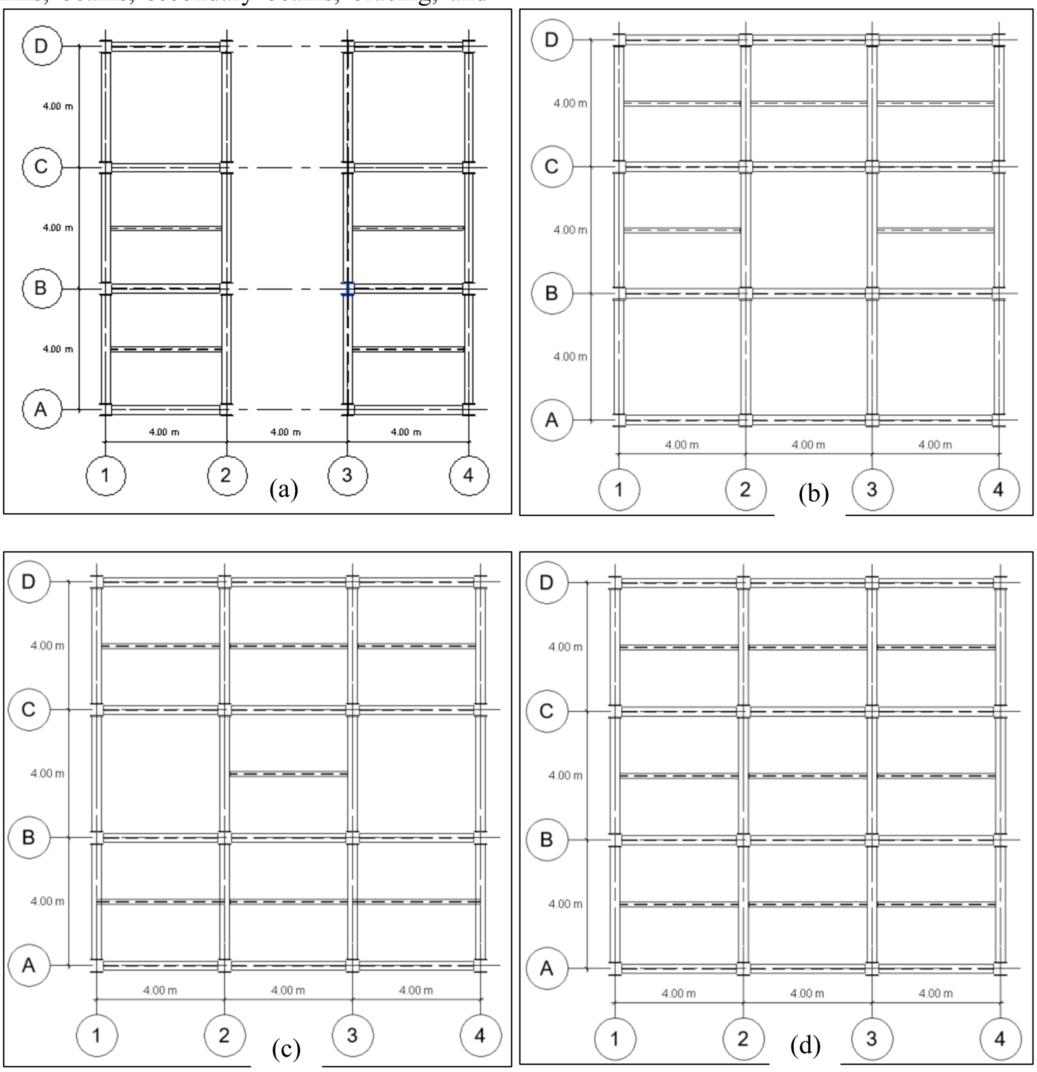

Fig. 1. Building layout: (a) first floor, (b) second, third, and fourth floors, (c) fifth floor, (d) roof floor.

Four structural models were developed in ETABS to assess the influence of bracing configurations on seismic behavior of structure, as illustrated in Fig.2. They were also considered to perform different structural response that account for the torsional, stiffness and shear distribution. Model A (Fig. 2a) represents a Moment Resisting Frame (MRF) for the baseline to measure the effect of bracing installation. Model B, C, and D were analyzed as EBF with the bracings were positioned in different configuration. In Model B (Fig. 2b), the bracing was installed continuously along the exterior perimeter bays on all four sides of the building. Model C (Fig. 2c) concentrated the bracing at the building corners whereas Model D (Fig. 2d) positioned the bracing at the midpoints of each exterior bay.

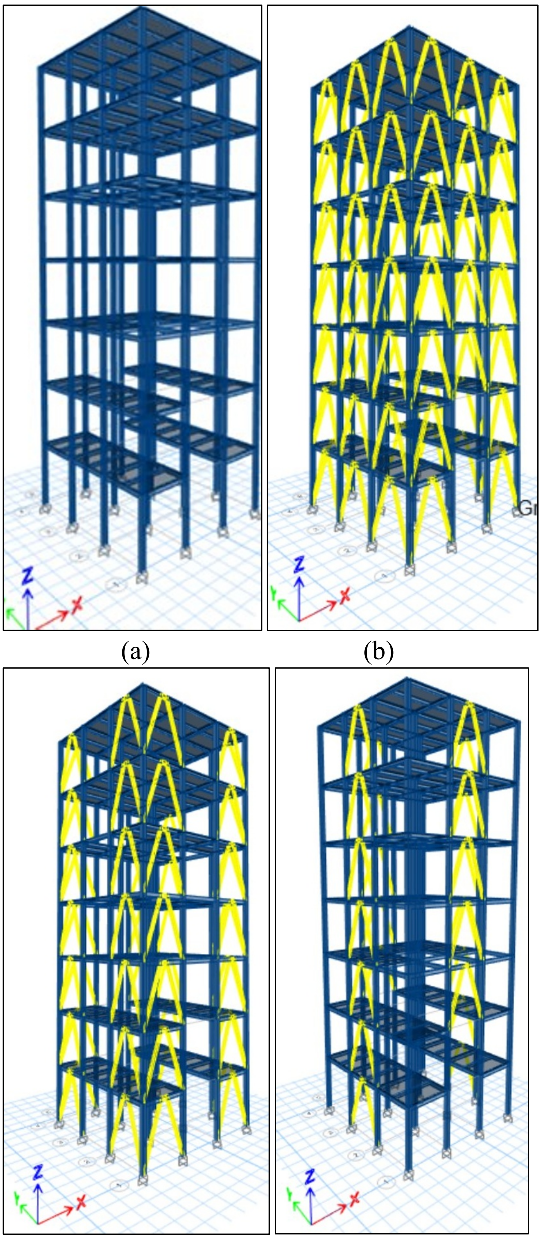

(a) (b)

(c) (d)

Fig. 2. The 3D observed models

2.2 Pushover analysis and fragility curve

After confirming that the structures satisfied the strength and serviceability criteria, non-linear pushover analysis was conducted to evaluate their seismic performance. This analysis produces a capacity curve, illustrating the relationship between the base shear and roof displacement. From this curve, essential performance parameters were obtained such as yield displacement (Δ_y), ultimate displacement (Δ_u), spectral displacement (S_d). These parameters were then used to determine the structure's performance levels in accordance with seismic performance FEMA 356 namely Immediate Occupancy (IO), Life Safety (LS), Damage Control (DC), Collapse Prevention (CP).

Subsequently, the seismic performance was further evaluated through the development of fragility curves utilizing the previously derived key parameters [13]. This methodology integrates pushover analysis results with probabilistic seismic demand to estimate the probability of exceeding different structural damage states categorized as slight, moderate, extensive, and complete. Furthermore, the spectral displacement (S_d) was derived from maximum roof displacement (Δ_{roof}), the modal participation factor (Γ). and first modal displacement at roof (ϕ), as expressed in Eq 1.

$$S_d = \frac{\Delta_{roof}}{\Gamma.\phi} \tag{1}$$

The fragility function in Eq.2 is developed by defining the intensity measure and modelling it using a lognormal cumulative distribution, where DS denotes the damage state, λ represents median displacement and β is standard deviation obtained from HAZUS value.

$$P[DS|S_d] = \phi\left(\frac{\ln(S_d) - \ln(\lambda)}{\beta}\right) \tag{2}$$

The findings derived this methodology form the comprehensive discussion and assessment nonlinear behaviour, ductility, and overall resilience of the structure under varying levels of spectral displacement.

3 Result and discussion

3.1 Interstory drift

Figure 3 illustrates that Model A exhibits the largest inter-story drift, reaching 23.087 mm, whereas Model B demonstrates the smallest. Overall, the inter-story drift values for all models remain with the permissible limits, remaining below the maximum allowable drift by SNI 1726:2019.

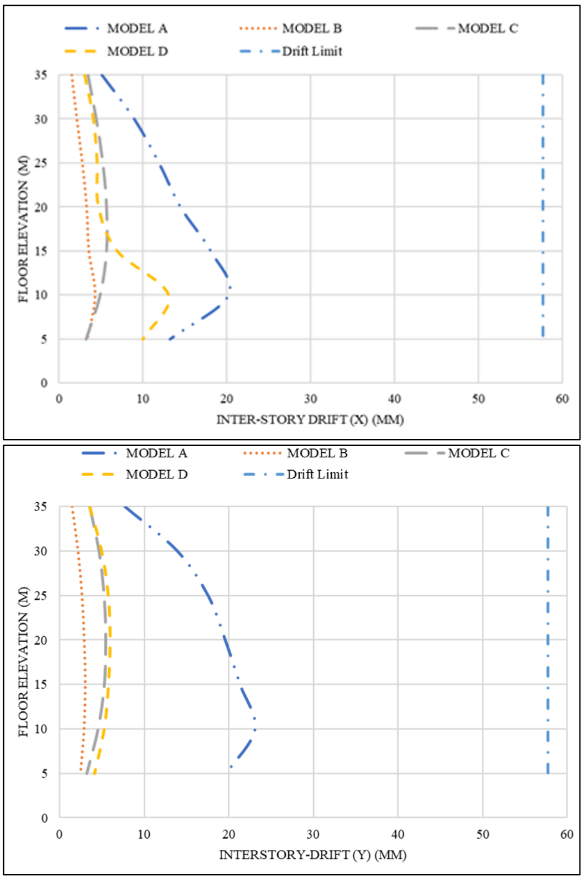

Fig. 3. Inter-story drift at x and y direction

The addition of eccentric bracing in Model B, C, and D significantly reduced the lateral displacement compared to moment frame Model A. Model B achieves the highest reduction of approximately 87%, attributed to the continuous placement of eccentric bracing along the building perimeter, which increase global lateral stiffness and distributes seismic forces more uniformly. Model C recorded an 83% reduction, benefiting from corner bracing that provides localized stiffness but less effective force distribution. Meanwhile, Model D obtained a 79% reduction due to its mid-span bracing arrangement, which improves stiffness at central bays but results in less lateral restraint at the corners. These results indicate that the configuration and distribution of eccentric bracing strongly influence the overall seismic performance.

3.2 Pushover analysis and structural performance

After the verification was completed, all models were analyzed using pushover analysis. The results from the ETABS analysis is capacity curves that show the relationship between displacement and base shear. For more clarity, the strength, stiffness, and ductility of each model with model A as the benchmark are shown in Tables 2 and 3.

The structural strength is determined by the magnitude of the base shear at the ultimate limit state that the structure can withstand before failure occurs. From Tables 2 and 3, it can be seen that the model with the highest strength is model B when viewed from both the X and Y directions. This can be observed from the strength percentage of model B compared to model A, which is 114% in the X direction and 143% in the Y direction.

Table 2. Strength, stiffness, and ductility at x direction

Model	Strength (kN)	Stiffness (kN/m)	Ductility
A	154966,541	464,013	2,007
B	176777,729	2369,627	2,827
C	170825,200	1502,566	2,116
D	151412,116	691,618	2,466

Table 3. Strength, stiffness, and ductility at y direction

Model	Strength (kN)	Stiffness (kN/m)	Ductility
A	128748,421	269,804	1,249
B	183864,014	2603,670	1,424
C	139627,918	1391,624	1,941
D	120966,567	859,968	3,099

Structural stiffness is calculated by dividing the base shear at the first yield point by the displacement at the first yield point. Visually, using the curve, stiffness can be assessed by the steepness of the structure's capacity curve or the initial angle of the curve relative to the x-axis. Based on Fig. 4 and Fig. 5, the curve for model B has a greater slope than the other models. The stiffness percentage of model B compared to model A reaches 965%, while model D has the lowest stiffness compared to model A, at 318%. It can be concluded that the use of bracing increases the stiffness of the building structure. The stiffer the structure, the smaller the displacement, thereby enhancing comfort during an earthquake.

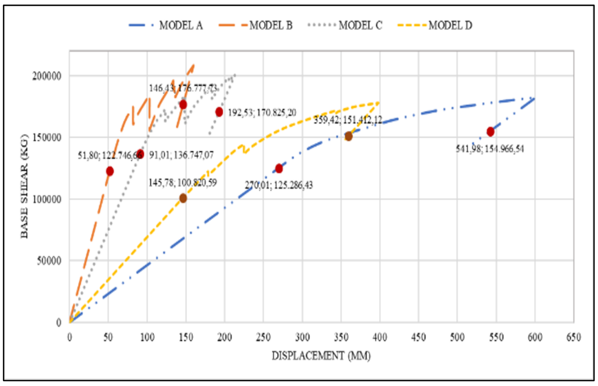

Fig. 4. The capacity curve and performance point at x-direction

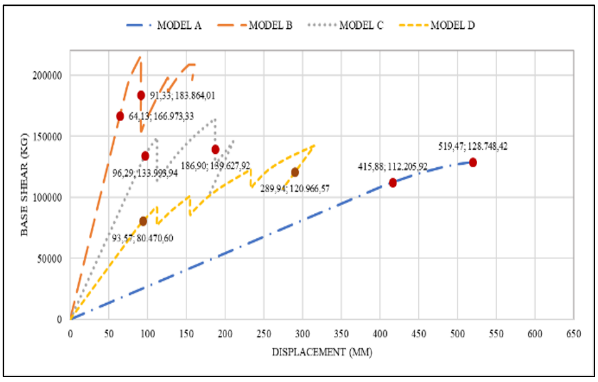

Fig. 5. The capacity curve and performance point at y-direction

Structural ductility is obtained from the ratio of displacement at the ultimate limit state to the displacement at the first yield point. For the X direction, the braced structure with the highest ductility is model B, with 141% of model A, while in the Y direction, it is model D with 248% of model A. However, overall, all models show an increase in ductility compared to model A. A ductile structure can undergo significant deformation before reaching the failure limit or collapse.

Therefore, it can be concluded that the use of eccentric bracing in buildings with a steel frame structural system has a significant impact on the strength, stiffness, and ductility of the structure, which is proportional to the amount of eccentric bracing used in the building.

The target displacement value and base shear at the target displacement are needed to determine the performance level of the structure. The FEMA 356 displacement target curve is used to determine the displacement targets for assessing the structural performance level. The structural performance level is determined in both the X and Y directions.

Table 4. Performance level

Model	Drift Percentage (%)		Performance Level	
	X	**Y**	**X**	**Y**
A	1,218	1,718	LS	CP
B	0,434	0,395	IO	IO
C	0,618	0,678	LS	LS
D	1,074	0,921	LS	LS

Table 4 provides information about models B, C, and D are at higher performance levels compared to model A, which is at the Collapse Prevention (CP) level. Model B is at the Immediate Occupancy (IO) level, while models C and D are at the Life Safety level. At the IO level, the building experiences structural damage that is not significant. Non-structural components remain functional and in place. The building can still be used without disruption from repair issues. The risk of casualties at this performance level is very low. At the Life Safety level, the building sustains structural damage that is not excessively severe. Non-structural components may be damaged and no longer functional, but the building still retains adequate collapse prevention capability. Therefore, it can be concluded that the configuration of eccentric bracing in the exterior frame of a steel-framed building affects the structural performance level.

3.3 Probability of exceeding damage

Table 5 presents the comparison of roof displacement and spectral displacement values at both yield and ultimate point for all structural models. The parameters were obtained from the pushover analysis by considering first mode participation factor and associated HAZUS values for MRF and EBF.

Table 5. Spectral displacement at yield and ultimate

Model	Δ_{roof} (yield) (mm)	Δ_{roof} (ult) (mm)	S_d (yield) (mm)	S_d (ult) (mm)
A	61,6	85,2	49,28	68,18
B	35,2	70	78,2	155,5
C	28	43,2	80	123,43
D	40,1	75,8	86,8	162,7

The fragility curves shown in Fig. 6 and Fig. 7 illustrated the probability of exceeding damage states (slight, moderate, extensive, and complete) as a function of spectral displacement. These curves were derived from pushover analysis results, incorporating parameters in Table 6. Each curve represents a different EBF configuration, enabling a comparative assessment of their seismic performance.

In slight damage, Model A (MRF) showed the earliest onset of slight damage, with spectral displacement around 30-37 mm, while Model B, C, and D follow sequentially at higher displacements 50-60 mm. This indicates that Model A is the most flexible reaching the initial yielding earlier, while Model C and D exhibit greater stiffness and delay slight damage event. In moderate damage, a similar trend is observed. Model C and D experience delayed moderate damage at 80-90 mm. The gap of the curves demonstrated that configuration B, C, and D are stiffer and can resist greater deformation before experiencing inelastic states.

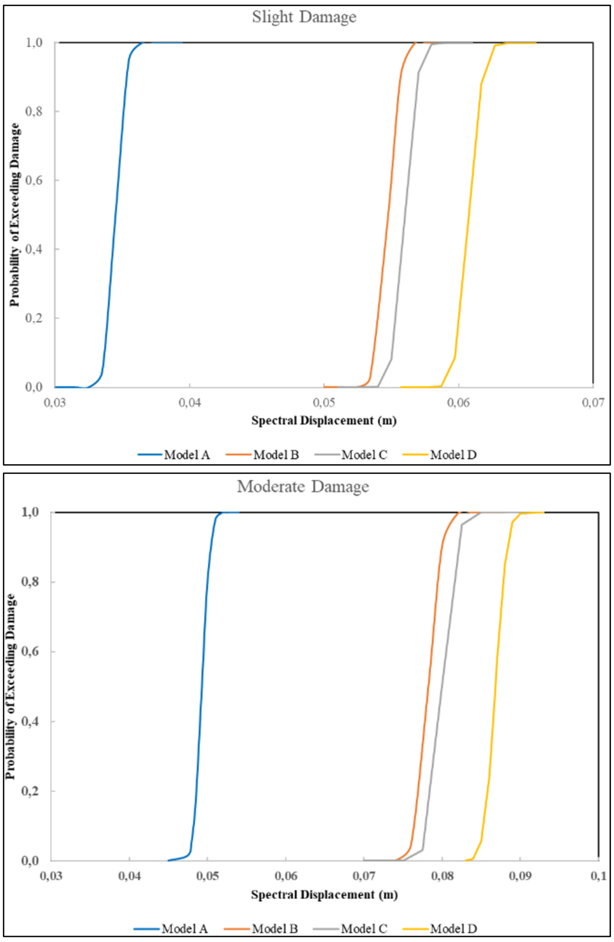

Fig. 6. The fragility curve of slight and moderate damage

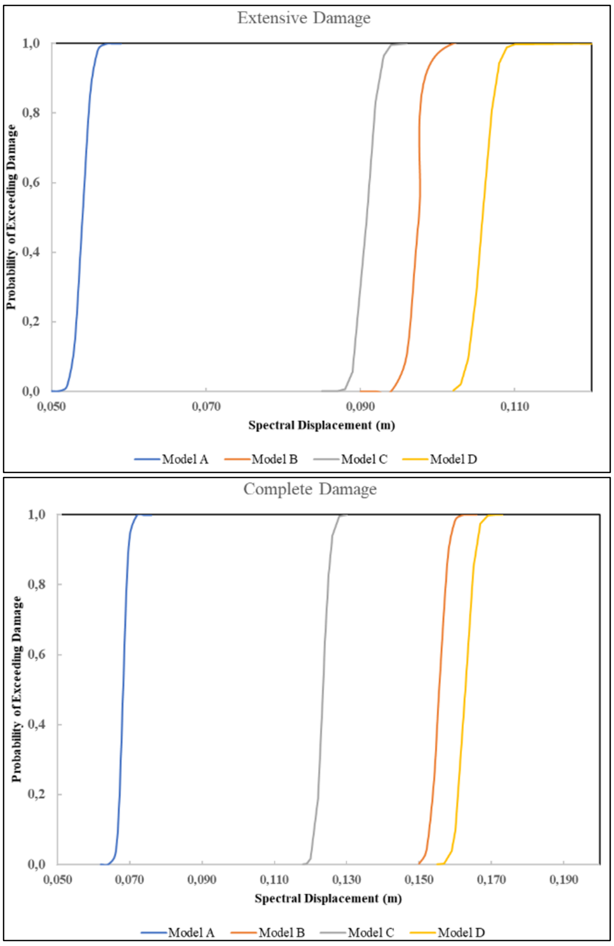

Fig. 7. The fragility curve of extensive and complete damage

However, in extensive and complete damage, a significant change was observed between Model B and C. Model B reached the extensive and complete damage respectively at spectral displacement of 95 mm and 120 mm, while Model C experienced it at 105 mm and 150 mm. Although Model D experienced those states at 110 mm and 170 mm, this finding indicates that Model B, despite demonstrating superior stiffness and smaller drift at lower performance levels, exhibits lower ductility capacity compared to Model C and Model D. The larger displacement capacity of Model C and D reflects its ability to undergo greater inelastic deformation before failure, suggesting a more gradual energy dissipation mechanism and enhanced structural resilience under severe seismic excitation.

4 Conclusion

Based on the analysis of all models in terms of inter-story drift, strength, stiffness, ductility, and structural performance level, it can be concluded that Model B represents the most optimal configuration of eccentric bracing steel frame. Model B maintain inter-story drift within the allowable limits, exhibits the highest strength and stiffness, although it demonstrates the adequate ductility by achieving Immediate Occupancy (IO) performance level, however, at extensive and complete damage states, Model B could not exhibit higher ductility compared to Model C and D that make serviceability demand is considered for Model B.

In terms of Life Safety (LS) performance, Model D serves the higher ductility compared to Model C, although Model C performs good stiffness and strength, for the collapse prevention under strong earthquake, Model D could be effective option due to better deformation under ultimate conditions by performing optimum energy dissipation.

This research is funded by '*Lembaga Penelitian dan Pengabdian Masyarakat* (LPPM) Universitas Andalas' through '*Penelitian Skripsi Sarjana'* with contract number 240/UN16.19/PT.01.03/PSS/2024.

References

1. Masrilayanti, Y. A. Hasibuan, R. Kurniawan, J. Sunaryati, and R. Aidil Fitrah, Performance evaluation of high-rise apartment building using pushover analysis. in E3S Web of Conferences **429** (2023). https://doi.org/10.1051/e3sconf/202342905024
2. M. Saravanan, R. Goswami, and G. S. Palani, Replaceable fuses in earthquake resistant steel structures: A review. Kor. Soc. of St. Cons. **18** (2018). https://doi.org/10.1007/s13296-018-0035-9
3. R. A. Fitrah and Masrilayanti, Seismic performance of special steel moment resisting frame building with consideration of setback irregularities. in AIP Conference Proceedings **2691** (2023). https://doi.org/10.1063/5.0114899
4. R. A. Fitrah, D. I. Mazni, W. Pratiwi, and Z. A. Jauhari, Seismic assessment of irregularities in steel special moment resisting frame with asymmetric-plan building (case study: Gedung D - Universitas Dharma Andalas). IOP Conf. Ser.: Earth Environ. Sci. **708** (2021). http://doi.org/10.1088/1755-1315/708/1/012007
5. V. Mohsenian, R. Filizadeh, I. Hajirasouliha, and R. Garcia, Seismic performance assessment of eccentrically braced steel frames with energy-absorbing links under sequential earthquakes. J. of Buil. Eng. **33** (2021). https://doi.org/10.1016/j.jobe.2020.101576
6. A. Hammad and M. A. Moustafa, Numerical analysis of special concentric braced frames using experimentally-validated fatigue and fracture model under short and long duration earthquakes. Bull. of Earth. Eng. **19**(1), 287–316 (2021). https://doi.org/10.1007/s10518-020-00997-8
7. M. S. Khan, A. Basit, M. Rizwan, and N. Ahmad, Seismic fragility functions for RC As-built and eccentric steel brace frames. Structures **50**, 1338–1352 (2023). https://doi.org/10.1016/j.istruc.2023.02.104
8. M. Bosco, Influence of uncertainties on the seismic performance assessment of chevron braced frames. Eng. Struct. **294** (2023). https://doi.org/10.1016/j.engstruct.2023.116594

9. J. Xu, S. L. Wang, H. S. Mohamed, J. Han, Z. Han, J. Tu, and Z. Li, Seismic performance of shear energy dissipation beams in d-shaped eccentrically braced steel frames. J. Constr. Steel Res. **180** (2021). https://doi.org/10.1016/j.jcsr.2021.106584
10. M. N. Wijaya, L. Susanti, and F. P. Pinontoan, Comparison of strain histories on reinforced concrete eccentric braced frame (EBF) with vertical and horizontal link. Rek. Sip. **19**(2) 169–177 (2025). https://doi.org/10.21776/ub.rekayasasipil.2025.019.02.5
11. A. G. Ureña, R. Tremblay, and C. A. Rogers, Earthquake-resistant design of steel frames with intentionally eccentric braces. J. Constr. Steel Res. **178** (2021). https://doi.org/10.1016/j.jcsr.2020.106483
12. J. Li, W. Wang, and P. Li, Development, testing and performance evaluation of steel beam-through framed connections with curved knee braces for improving seismic performance. J. Constr. Steel Res. **179** (2021) https://doi.org/10.1016/j.jcsr.2021.106552
13. K. T. Htay, J. Tanjung, Masrilayanti, M. Olivia, F. M. Nazri, and M. Bur, A proposed fragility curve based on PO-ID hybrid analysis for seismic assessment performance of the reinforced concrete continuous bridges in earthquake prone area. Buildings **14**(12) (2024) https://doi.org/10.3390/buildings14123875.